5

Semi-empirical model for axial segregation in metal-halide lamps

Abstract.
Diffusive and convective processes in the metal-halide lamp cause an unwanted non-uniform distribution of the radiating metal additive (Dy in our case), which results in colour separation. The axial segregation has been described by E. Fischer [J. Appl. Phys. **47**, 2954 (1976)] for infinitely long lamps with a constant axis temperature. However, for our lamps this is not valid. We propose a semi-empirical extended model. The density inhomogeneity gives a measure for the non-uniformity of the Dy density distribution in the lamp. As an example, this parameter is calculated for some measurements obtained by imaging laser absorption spectroscopy.

This chapter has been adapted from [A.J. Flikweert, M.L. Beks, T. Nimalasuriya, G.M.W. Kroesen, M. Haverlag, J.J.A.M. van der Mullen and W.W. Stoffels, *Semi-empirical model for axial segregation in metal-halide lamps*, J. Phys. D: Appl. Phys. **41** (2008) issue 18].

Figure 5.1: (printed in colour in figure 1.3) The burner of a MH lamp (10 mg Hg, 4 mg DyI_3, input power 150 W). Colour segregation is clearly visible [37, 67].

5.1 Introduction

High intensity discharge (HID) lamps have a high efficiency (up to 40%) and a good colour rendering index [3, 21–26, 35, 42]. They are for instance used for shop lighting, city beautification and street lighting. A commonly used HID lamp is the metal-halide (MH) lamp. These arc discharge lamps contain a buffer gas (usually mercury) and additives that act as prime radiator in the visible spectrum. In our case we use dysprosium iodide (DyI_3) as salt additive. This additive increases the efficiency and colour rendering of the lamp.

Colour segregation is observed when the lamp is burning in the vertical position. The colour segregation originates from the segregation of the additives. This limits the lamp design for application. Figure 5.1 shows the lamp when burning in the vertical position. The Dy atoms stay mainly at the bottom, where we see bluish-white light. The bluish colour at the top is caused by Hg atoms.

The convection of the buffer gas Hg in HID lamps was described by Kenty [68] and Elenbaas [53]. The segregation of additives in MH lamps was described by Zollweg [23]. His theory is based on single cell convection of the buffer gas and radial diffusion of the additives. E. Fischer [28] developed a model based on the diffusion–convection mechanism in vertically operated lamps. The diffusion is based on the chemical equilibrium between the salt molecules and the atoms. His model describes the amount of segregation as a function of the amount of convection (figure 5.2). The amount of Dy decreases exponentially with the axial position in the lamp. The amount of convection increases among others with Hg pressure, input power, aspect ratio of the burner and gravity [23, 28, 37, 69]. To vary the amount of convection, in the past several experi-

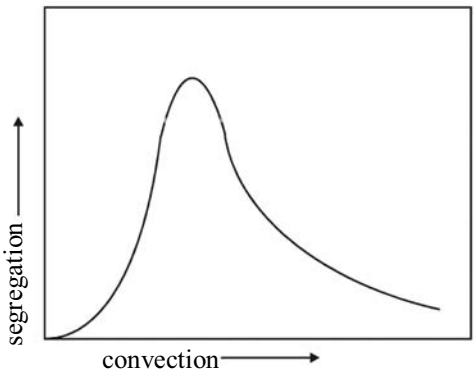

Figure 5.2: The Fischer curve shows the axial segregation as a function of the amount of convection [28, 32, 67]. The lamps we use are around the maximum of the curve.

ments under varying gravity conditions have been carried out: in the lab ($1g$, where g is the gravity at earth: 9.81 m s^{-2}; see chapter 2 [32, 34, 35, 50]), the International Space Station ($0g$) [41], during parabolic flights (0–$2g$; chapter 3 [33]) and in a centrifuge (1–$10g$; chapters 4 and 8 [37–39]).

E. Fischer assumes an infinitely long lamp with a constant axis temperature and no end effects of the convection flow. However, our lamps have a burner length of 10–30 mm and a diameter between 4 and 8 mm [27]. For these lamps, the axis temperature is not constant. Therefore, the Fischer theory cannot be applied to our lamps.

The aim of this chapter is to propose a semi-empirical axial segregation model and to introduce a new parameter that expresses the degree of inhomogeneity in the axial direction of any plasma parameter. First, the transport phenomena in the MH lamp are summarized. The axial segregation model as described by E. Fischer is discussed briefly. This model is only valid for a constant axis temperature. Whereas Fischer predicts an exponentially decreasing Dy density as a function of the axial position, we observe that the Dy density from the bottom to the top first increases, and next decreases. The increase is explained by the non-uniform temperature over the axis, which shifts the chemical equilibrium between atoms and molecules. The temperature distribution was obtained by numerical simulations [42, 70].

We introduce a new parameter: the density inhomogeneity. This parameter can be used to determine the inhomogeneity of the additives, which is independent of the measurement technique and lamp geometry. To compare with earlier results [32, 38, 50], the segregation model of Fischer can be corrected for the temperature effect. This corrected axial segregation parameter is only valid if the temperature effect is not dominant. We give some examples of the density inhomogeneity and the corrected axial segregation parameter for our lamps.

5.2 Transport in the MH lamp

The theory of the transport phenomena in the MH lamp has been described in earlier publications [28, 32, 33, 67]. For clarity, the most important part is summarized here.

After ignition of the lamp, Hg evaporates first. Next, during heat up, the salt (DyI_3) evaporates and enters the arc. Because of the temperature gradient (∼5500 K at the centre and ∼1200 K at the wall) in combination with gravity, we have convection. The gas in the hot centre moves upwards, whereas the gas at the cooler wall moves downwards.

Due to the large temperature gradient in the radial direction, a multi-step process of dissociation of the DyI_3 molecules takes place when moving from the wall to the centre [32, 50, 70]. In addition, in the hot centre ionization of the Dy atoms takes place [31]. The lighter atoms and ions diffuse faster outwards than the heavier molecules move inwards. This difference in diffusion velocities leads to a hollow radial profile of the elemental Dy pressure; this is called radial segregation. In addition, the density in the centre is lower due to the ideal gas law $p = nkT$.

The chemical equilibrium between DyI_3 molecules and atoms is given by

$$\mathrm{DyI_3} \rightleftarrows \mathrm{DyI_2} + \mathrm{I} \rightleftarrows \mathrm{DyI} + 2\mathrm{I} \rightleftarrows \mathrm{Dy} + 3\mathrm{I}. \tag{5.1}$$

The equilibrium shifts to the right when the temperature is increased. When the temperature is increased even further, ionization of Dy atoms takes place:

$$\mathrm{Dy} + \mathrm{e} \rightleftarrows \mathrm{Dy^+} + \mathrm{e} + \mathrm{e}. \tag{5.2}$$

The partial pressures of the different particles were calculated as a function of temperature, under assumption of local thermodynamical equilibrium (LTE) and for a fixed cold spot temperature of 1100 K [56]. These pressures are shown in figure 5.3.

While the atoms are moving outward caused by diffusion, they are dragged downward by the convection flow. As a result, the atoms stay at the bottom of the lamp. The combination of convection and diffusion causes an axial gradient in atomic Dy density: axial segregation appears. When the diffusion and convection are in the same order of magnitude, maximal axial segregation occurs. In the two limiting cases, when the convection is very small, or when the convection is much stronger than the diffusion, no axial segregation is present.

5.3 Axial segregation

An axial segregation model based on diffusion and convection has been proposed by E. Fischer [28]. This model, which is valid for an infinitely long lamp burning in the vertical position, is repeated briefly in section 5.3.1. The Fischer model assumes a constant axis temperature. However, our lamps are not infinitely long and have an

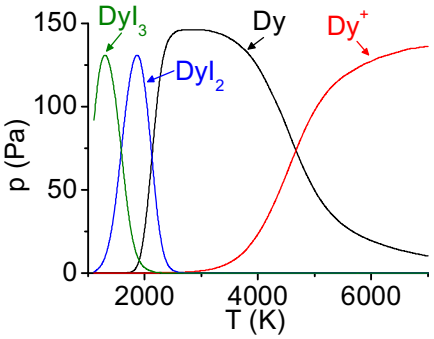

Figure 5.3: Theoretical pressures of Dy atoms, ions and molecules as a function of temperature, at a fixed cold spot temperature of 1100 K. The DyI pressure is small and has been omitted for clarity [56, 71].

axial temperature gradient. Section 5.3.2 shows that the atomic Dy density determined by Saha [31] and Guldberg–Waage (chemical equilibrium) is not constant over the axial position in the lamp, due to the temperature variation over the axis. The temperature profile was obtained by numerical simulations [42, 70].

Section 5.3.3 introduces a new parameter which describes the density inhomogeneity of additives in the lamp. This parameter is normalized and can be used for different lamp geometries and for different particles in the lamp. When the temperature effect is combined with the Fischer theory, we can define a corrected segregation parameter. This is described in section 5.3.4. When the temperature effect is more important than the segregation according to Fischer, the corrected segregation parameter is not valid anymore and only the inhomogeneity parameter can be used to characterize the lamp.

5.3.1 Fischer model

E. Fischer [28] developed a diffusion–convection axial segregation model for an infinitely long lamp, burning in the vertical position. He assumes a parabolic radial temperature profile that is independent of the axial position. The convection profile in the lamp, which is the convection profile of the buffer gas in all MH lamps [38], is calculated using the Navier–Stokes equation. The axial convection speed v_z is described by [42, 53, 70]

$$v_z \sim p_{\mathrm{Hg}} R^2 g, \tag{5.3}$$

where p is the pressure, R the burner radius and g gravity. The convection speed v_z also increases with increasing lamp input power P since the temperature gradient increases [23].

Fischer solved the transport problem. For the Dy density $n_{\mathrm{Dy}}(r, z)$ (m^{-3}) in the

lamp this gives

$$n_{\mathrm{Dy}}(r,z) = n_{\mathrm{Dy},0}(r)\exp\left(-\lambda z\right), \tag{5.4}$$

where r is the radial position in the lamp, $n_{\mathrm{Dy},0}(r)$ is the Dy density at the bottom of the lamp at the radial position r and λ is the axial segregation parameter.

We want to average out noise in the measurement data, and therefore the Dy density is radially averaged. The radially integrated Dy density $N_{\mathrm{Dy}}(z)$ is given by

$$N_{\mathrm{Dy}}(z) \equiv \int_0^R n_{\mathrm{Dy}}(r,z)\cdot 2\pi r \mathrm{d}r, \tag{5.5}$$

where R is the radius of the burner. The density $N_{\mathrm{Dy}}(z)$ is the amount of Dy present in the cross section of the lamp at the axial position z, per unit length (m^{-1}).

When we radially integrate equation (5.4) we obtain

$$\begin{aligned} N_{\mathrm{Dy}}(z) &= \exp\left(-\lambda z\right)\cdot\int_0^R n_{\mathrm{Dy},0}(r)\cdot 2\pi r\mathrm{d}r \\ &\equiv N_{\mathrm{Dy},0}\exp\left(-\lambda z\right). \end{aligned} \tag{5.6}$$

The Fischer curve, which gives the amount of axial segregation λ as a function of the amount of convection, is shown in figure 5.2. The segregation is maximal when the convection is in the same order of magnitude as the diffusion. In the two limiting cases, when the convection is much smaller than diffusion, or when the convection is dominant over diffusion, we have [28, 33, 37]

$$\begin{aligned} \lambda \sim\ & p_{\mathrm{Hg}}^2 R^2 g && \text{for small } p_{\mathrm{Hg}},\ R \text{ or } g, \text{ and} \\ \lambda \sim\ & \left(p_{\mathrm{Hg}}^2 R^2 g\right)^{-1} && \text{for large } p_{\mathrm{Hg}},\ R \text{ or } g. \end{aligned} \tag{5.7}$$

5.3.2 Temperature influence on atomic Dy density

The Fischer model of axial segregation of the elemental Dy is valid for the infinitely long vertically burning lamp only. He assumes a constant axial temperature and no electrode effects. However, in real life the lamps are finite size. Therefore, we need to take into account an axial temperature gradient. Furthermore we want to have a model that describes the axial segregation of atomic Dy, whereas the Fischer model describes elemental densities. To bridge the gap between the Fischer model and the COST reference lamps (see section 1.3.1 and [27]) used in our experiments [32, 33, 35, 37, 39, 42, 67], we develop a new semi-empirical model.

Our lamps have an axial temperature gradient. When the temperature changes, the chemical equilibrium between DyI_3 molecules and Dy and I atoms shifts. The densities of the different particles in equation (5.1) were calculated as a function of temperature, under assumption of Local Thermodynamical Equilibrium (LTE) and for a fixed cold spot temperature of 1100 K [56]. The cold spot of the lamp is located at the

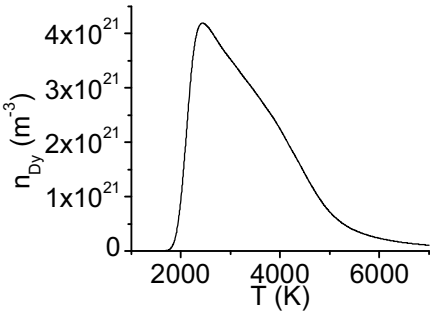

Figure 5.4: Atomic Dy density (all states) as a function of temperature T, at a fixed cold spot temperature of 1100 K. The decrease at a higher temperature is caused by the ionization of the Dy atoms.

bottom, where the salt pool is located. At low temperature we mainly have molecules, whereas at high temperature mainly ions are present. Somewhere in between we have the temperature where the atomic Dy density (and thus the radiative output) is the highest. Figure 5.4 shows the atomic Dy density as a function of temperature.

For a lamp of 20 mm height and 8 mm diameter Beks *et al* [70] carried out numerical simulations to calculate the temperature profile $T(r, z)$ in the lamp burner under various gravity conditions. The temperature profile for a lamp with 5 mg Hg, 150 W lamp input power, at $1g$ is shown in figure 5.5(a). From this temperature profile the radial atomic Dy profile $n_{\mathrm{Dy}}(r, z)$ is calculated (figure 5.5(b)). This profile shows the density profile determined by the Saha and Guldberg–Waage equilibria; the calculated density at each position is only based on temperature, neglecting diffusion and convection effects. Taking the radially integrated atomic Dy density gives the curves shown in figure 5.6, for $1g$ and $10g$. At $10g$ the temperature varies more along the axis.

Due to the temperature influence, the Fischer parameter as discussed in section 5.3.1 is not valid anymore for our lamps. Therefore, a new parameter should be introduced to describe the axial segregation in the lamps.

5.3.3 Axial density inhomogeneity parameter

Fischer described the axial segregation by an exponential decay of the density in the axial direction. We introduce a new parameter to express the degree of inhomogeneity in the axial direction for any plasma parameter, which does not assume a particular shape for the axial profile.

In general, any lamp property can be described by $q(r, z)$. For the axial inhomogeneity of the lamp property $q(r, z)$ we first integrate over the cross section of the lamp

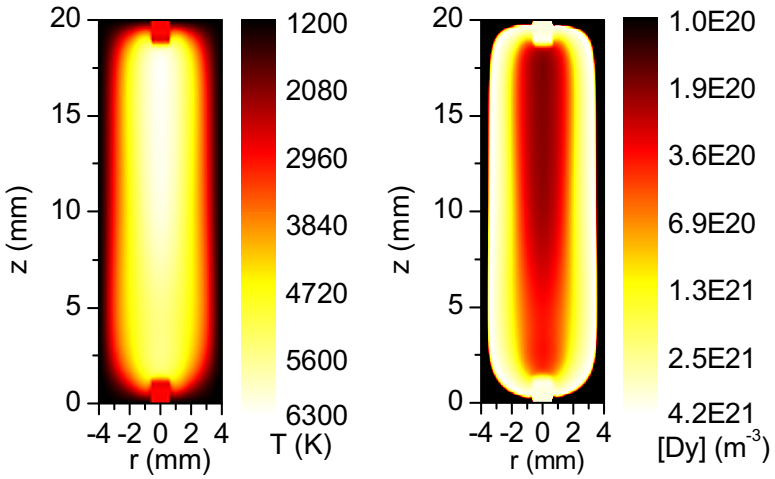

Figure 5.5: (a) Temperature profile $T(r, z)$ obtained by numerical simulations [42] for a lamp containing 5 mg Hg and 4 mg DyI_3, input power 150 W at $1g$.
(b) Radial atomic Dy density $n_{\mathrm{Dy}}(r, z)$ for a fixed cold spot temperature of 1100 K. This profile is based on LTE calculations and the calculated temperature profile of (a) and neglecting diffusion and convection effects.

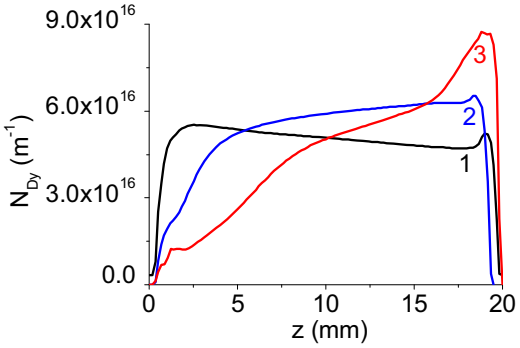

Figure 5.6: Radially integrated atomic Dy densities $N_{\mathrm{Dy}}(z)$, calculated from figure 5.5 by equation (5.5) for different amounts of mercury and gravity: (1) 5 mg Hg, $1g$; (2) 5 mg Hg, $10g$; (3) 10 mg Hg, $10g$. For these densities only the temperature profiles $T(r, z)$ are taken into account; segregation effects due to diffusion and convection have not been taken into account.

at axial position z:

$$Q(z) = \int_0^R q(r,z) \cdot 2\pi r \mathrm{d}r. \tag{5.8}$$

Next we normalize this property $Q(z)$ over the height:

$$\overline{Q} = \frac{1}{H}\int_0^H Q(z)\mathrm{d}z = \frac{1}{H}\int_0^H \left(\int_0^R q(r,z)\cdot 2\pi r \mathrm{d}r\right)\mathrm{d}z, \tag{5.9}$$

where H is the height of the lamp burner. Next the difference between the lamp property $Q(z)$ at position z and the average $\overline{Q}$ is calculated and normalized. This gives the axial inhomogeneity parameter α:

$$\alpha = \sqrt{\frac{1}{H}\int_0^H \left(\frac{Q(z)-\overline{Q}}{\overline{Q}}\right)^2 \mathrm{d}z}. \tag{5.10}$$

A value of $\alpha = 0$ means that lamp property $Q(z)$ is homogeneous over the lamp height H.

The axial inhomogeneity parameter α is generally applicable and dimensionless, in contrast to the Fischer parameter λ. Therefore, α is independent of the measurement technique and lamp geometry. This parameter can, among others, be used for imaging laser absorption spectroscopy (ILAS) measurements [72], where we can use α to describe the atomic Dy distribution over the lamp. Furthermore, it can be used for optical emission spectroscopy measurements with an axial intensity profile, where α is the intensity inhomogeneity. The parameter is normalized for the length of the burner and can be used to compare different lamp geometries of the same type (for example, we can compare different MH lamps or we can compare different ultra high pressure (UHP) lamps).

The inhomogeneity parameter α can, for example, be used to describe the density inhomogeneity of the ground state atomic Dy densities that are measured by ILAS: in equations (5.9) and (5.10), $Q(z)$ is substituted by $N_{\mathrm{Dy}}(z)$. When the temperature influence (section 5.3.2) is negligible and the Fischer model is valid, a relation can be found between the generic density inhomogeneity α and the particular Fischer parameter λ. When $Q(z) = N_{\mathrm{Dy}}(z)$ in equation (5.10) is substituted by the Fischer formula (equation (5.6)) we obtain:

$$\alpha(\lambda) = \sqrt{\frac{\lambda H}{2}\cdot\frac{1+\exp\left(-\lambda H\right)}{1-\exp\left(-\lambda H\right)} - 1}. \tag{5.11}$$

If $\lambda H \gtrsim 1$, we get $\alpha^2 \sim \lambda$ and the dependences as given in equation (5.7) are also valid for α^2.

5.3.4 Corrected Fischer parameter

To compare with earlier measurements where Fischer parameters were obtained, we introduce a corrected Fischer parameter which takes the temperature influence into account. This corrected parameter should follow the dependence of p, g and P as given in equation (5.7).

The axial temperature profile in the lamp determines the chemical equilibrium and the shift between atoms and ions (section 5.3.2). Beks *et al* obtained the temperature profiles of the MH lamp by numerical simulations as shown in figure 5.5(a). The density $N_{\mathrm{Dy}}(z)$ from the simulations without convection and diffusion, thus only determined by the local temperature, is given in figure 5.6. To correct the Fischer parameter, we want to introduce a correction term $T_{\mathrm{cor}}(z)$ for equation (5.6), that follows the same trend as the N_{Dy} curves in figure 5.6. Hereto we propose the following semi-empirical equation:

$$T_{\mathrm{cor}}(z) = \left(1 - \exp\left(-a\,(z-b)^2\right)\right) \cdot (1 + cz)\,, \tag{5.12}$$

where a, b and c are fitting parameters. This correction function describes the rising part of the curve by the exponential term $(1-\exp(-a(z-b)^2))$. This rise is caused by the increasing temperature from the bottom electrode upwards, which first increases the atomic Dy density as seen in figure 5.4. When the temperature increases further, the atomic Dy density decreases because of ionization. This is described by the second term $(1+cz)$. The combination of these two terms that describe the rising and decreasing parts describes well the trends of the curves in figure 5.6.

When the temperature correction of equation (5.12) is taken into account, the segregation parameter λ introduced by E. Fischer (equation (5.4)) can be corrected for the temperature effect. This corrected Fischer parameter λ_{c} is used to compare measurements with the theory for lamps with constant axial temperature as described by Fischer.

The ground state atomic Dy density $N_{\mathrm{Dy}}(z)$ is a product of the Fischer equation and the temperature correction $T_{\mathrm{cor}}(z)$:

$$\begin{aligned} N_{\mathrm{Dy}}(z) &= N_{\mathrm{Dy},0} \cdot \exp\left(-\lambda_{\mathrm{c}} z\right) \cdot T_{\mathrm{cor}}(z) \\ &= N_{\mathrm{Dy},0} \cdot \exp\left(-\lambda_{\mathrm{c}} z\right) \cdot \left(1 - \exp\left(-a\,(z-b)^2\right)\right) \cdot (1+cz)\,. \end{aligned} \tag{5.13}$$

This equation defines the corrected segregation parameter λ_{c}. When the temperature correction $T_{\mathrm{cor}}(z)$ is small, $\lambda_{\mathrm{c}} \approx \lambda$. The corrected axial segregation parameter can be obtained by fitting of, for example, ILAS measurements [37]. In this case the ground state atomic Dy density $N_{\mathrm{Dy}}(z)$ is experimentally determined and fitted by equation (5.13).

The quantitative model described in this section is valid for finite lamps, with an axial temperature gradient. The segregation parameter λ_{c} obtained from equation (5.13) is only applicable when the correction for the temperature (equation (5.12)) is

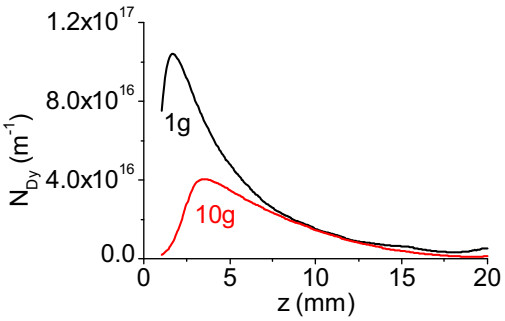

Figure 5.7: Radially integrated ground state atomic Dy for a lamp obtained by ILAS, at $1g$ and $10g$ (5 mg Hg, 4 mg DyI_3, P =148.4 W) [37]. The fit according to equation (5.13) is indistinguishable from the experimental data and therefore not shown.

smaller than the segregation according to Fischer (equation (5.4)). If the temperature effect on the atomic Dy density is greater than the segregation by Fischer, the obtained λ_c is inaccurate and does not give a measure for the axial segregation in the lamp. We can check this by calculating $\alpha(\lambda_c)$ by equation (5.11) and compare this value with α obtained directly from the measurement (section 5.3.3). The larger the difference between these two values, the larger the temperature effect is.

5.4 Example of fitting parameters for a measurement

The parameters α and λ_c (sections 5.3.3 and 5.3.4) have been obtained for a COST reference lamp (section 1.3.1) [27]. The lamp contains a starting gas (300 mbar Ar/Kr^{85}), 5 mg Hg as buffer gas (6 bar)[1] and 4 mg DyI_3 as salt additive. The diameter of the lamp is 8 mm and the height is 20 mm. The input power is $P = 148.4$ W. The gravity is varied between $1g$ and $10g$.

In figure 5.7 the radially integrated atomic Dy density N_{Dy} of the lamp is plotted as a function of the axial position z in the lamp. The figure shows that the density maximum shifts upwards for higher g. This is in agreement with figure 5.6, which shows that the Dy density also shifts upwards caused by the shift in the temperature.

For the curves shown in figure 5.7, the values for the density inhomogeneity are $\alpha = 1.05$ ($\alpha^2 = 1.10$) and $\alpha = 0.92$ ($\alpha^2 = 0.85$) at $1g$ and $10g$ respectively. The temperature dependence causes the maximum of the ground state atomic Dy density to shift upwards. It also affects the slope of the decreasing part in figure 5.7. For these two curves, the uncorrected segregation parameters are $\lambda = 0.23$ mm^{-1} and $\lambda = 0.16$ mm^{-1} at $1g$ and $10g$ respectively, whereas the corrected segregation parameters

[1] When the cold zones behind the electrodes are taken into account, the pressure is around 5 bar.

are $\lambda_c = 0.24$ mm^{-1} and $\lambda_c = 0.10$ mm^{-1} respectively. These values show a greater difference at $10g$ than at $1g$, because the temperature effect is also stronger at $10g$ than at $1g$. When the values of α^2 are compared with the segregation parameters λ_c, one sees that at $10g$ the segregation parameter is decreased compared to $1g$, whereas the density inhomogeneity is only decreased slightly. This difference is caused by the axial temperature gradient that is stronger at $10g$ than at $1g$ (figure 5.6), partially cancelling the lower Fischer segregation.

The influence of the temperature gradient is also seen when $\alpha(\lambda = \lambda_c)$ is calculated (equation (5.11)). We obtain 1.44 and 0.31 for $1g$ and $10g$ respectively. At $1g$ the measured density inhomogeneity (1.05) is somewhat smaller than one would expect from $\alpha(\lambda_c)$ (1.44), but at $10g$ the density inhomogeneity (0.92) is much larger than one would expect (0.31). This indicates that at $10g$ the temperature gradient along the axis has a strong influence on the density inhomogeneity.

5.5 Conclusions

We introduced the axial density inhomogeneity parameter α, which describes the axial inhomogeneity of the additive density for real lamps with an axial temperature gradient. This is an addition to the Fischer model, which describes the axial segregation of the metal additives in infinitely long lamps with a constant axial temperature profile. In our case the MH lamp, containing DyI_3 as salt additive, is not infinitely long and we have an axial temperature gradient. When the temperature changes, the chemical equilibrium between salt molecules, atoms and ions shifts. The radially integrated density of Dy atoms as a function of the axial position, determined by the Saha and Guldberg–Waage equilibria, has been obtained by temperature calculations from numerical modelling.

Two parameters have been introduced. Firstly, the density inhomogeneity α describes the inhomogeneity in the additive density. Secondly, the Fischer parameter has been corrected for the temperature influence. This gives the corrected axial segregation parameter λ_c and can only be obtained when the temperature influence is not dominant.

Finally, as an example, the parameters α and λ_c were calculated for two measurements obtained by ILAS. From these measurements, it is concluded that the temperature influence is much more pronounced for $10g$ than for $1g$. This is in agreement with the temperature calculations by the numerical simulations.

Acknowledgements

The authors are grateful to all participants in the ARGES project for their contributions, especially the General Technical Department of the Eindhoven University of Technology for building the centrifuge, and Senter-Novem (project EDI 03146), SRON [66] and the Dutch Ministries of Research and Education as well as Economic Affairs for funding the research.